Al-Farouk journal of sciences
Volume (2), Issue (4) (Spt, 2026)
ISSN: 3135-2359

مجلة الفاروق للعلوم
المجلد (2) العدد 4 سبتمبر 2026
ردمد: 3135-2359

# UNVEILING THE EFFICIENCY OF CARBONYL SULFIDE CAPTURE BY ORGANIC SOLVENTS: AN ELECTRON CORRELATION STUDY

**[1]Nizar Ramadan, [2]Mahmoud Abduesslam**
[1]Surman College of Since and Technology, Surman, Libya.
[2]Higher Institute of Science and Technology- Wadi Al-Ajal – Libya.
*Corresponding author, e-mail: nizar.r@scst.edu.ly

**Received: 08/9/2026 Revised: 13/9/2026 Accepted: 05/10/2026 Publication: 26/10/2026**

## Abstract

Natural gas plays a pivotal role in the global transition toward cleaner energy alternatives; however, the sustainable utilization of unconventional and contaminated reserves remains restricted by the presence of hazardous sulfur species. While conventional gas sweetening processes effectively reduce hydrogen sulfide ($H_2S$) levels, meeting stringent modern environmental regulations requires the comprehensive elimination of trace, less-reactive organosulfur contaminants, particularly carbonyl sulfide (COS). (COS) poses severe threats due to its high toxicity, pipeline corrosion potential, and tendency to poison industrial catalysts. To address the limitations of traditional alkanolamine absorption, Carbonyl Sulfide-Binding Organic Liquids (COS-BOLs) comprised of sterically hindered organic bases and linear alcohol co-solvents have emerged as highly tunable, efficient alternatives. Nevertheless, the precise molecular-level mechanisms and termolecular reaction kinetics governing these systems remain poorly understood. In this study, rigorous quantum mechanical calculations and electron correlation methods, including Density Functional Theory (DFT), were deployed to systematically investigate the efficiency of (COS) immobilization by organic solvent mixtures. Specifically, the termolecular, single-step reaction pathways between (COS) and key amidine or guanidine organic bases including 1,8-diazabicycloundec-7-ene (DBU), 1,5-diazabicyclonon-5-ene (DBN), 2-tert-butyl-1,1,3,3-tetramethylguanidine (BTMG), and 1,5,7-triazabicyclodec-5-ene (TBD) were mapped in the presence of various linear alcohols. By elucidating the dominant base effects and synergistic alcohol co-solvent behaviors through high-level electronic structure configurations, this work delivers crucial molecular insights necessary for the rational design and optimization of high-performance organic solvents for effective (COS) mitigation.

**Keywords:** Carbonyl Sulfide (COS) Capture; (COS-BOLs); Density Functional Theory (DFT); Termolecular Kinetics; Electron Correlation; Gas Sweetening.

الملخص

يلعب الغاز الطبيعي دوراً محورياً في التحول العالمي نحو بدائل الطاقة الأكثر نظافة؛ ومع ذلك، فإن الاستغلال المستدام للاحتياطيات غير التقليدية والملوثة يظل مقيداً بوجود مركبات الكبريت الخطرة. وفي حين أن عمليات تحلية الغاز التقليدية تنجح بفعالية في خفض مستويات كبريتيد الهيدروجين ($H_2S$) ، فإن تلبية اللوائح البيئية الحديثة والصارمة تتطلب الإزالة الشاملة لملوثات الكبريت العضوية الأثرية والأقل تفاعلية، ولا سيما كبريتيد الكربونيل .(COS) يشكل كبريتيد الكربونيل تهديداً جسيماً

نظراً لسميته العالية، وقدرته على إحداث التآكل في خطوط الأنابيب، وميله إلى تسميم الحوافز الصناعية. ولمعالجة قصور عمليات الامتصاص التقليدية بالالكانولامينات، ظهرت السوائل العضوية الرابطة لكبريتيد الكربونيل (COS-BOLs) ـ المكونة من قواعد عضوية معاقة فراغياً ومذيبات مصاحبة من الكحولات الخطية ـ كبدائل عالية الضبط والكفاءة. ومع ذلك، فإن الآليات الدقيقة على المستوى الجزيئي والحركية التفاعلية ثلاثية الجزيئات التي تحكم هذه الأنظمة لا تزال غير مفهومة بشكل كافٍ. في هذه الدراسة، تم تطبيق حسابات ميكانيكا الكم الصارمة وطرق ارتباط الإلكترونات، بما في ذلك نظرية الدالة الكثافية(DFT) ، للاستقصاء المنهجي لكفاءة احتجاز كبريتيد الكربونيل بواسطة مخلوطات المذيبات العضوية. وتحديداً، تم رسم مسارات التفاعل أحادية الخطوة وثنائية الجزيئات بين كبريتيد الكربونيل وقواعد عضوية رئيسية من الأميدين أو الجوانيدين ـ تشمل 1،8-diazabicycloundec-7-ene (DBU)، و 1،5-diazabicyclonon-5-ene (DBN)، و 2-tert-butyl-1,1,3,3-tetramethylguanidine (BTMG)، و 1،5،7-triazabicyclodec-5-ene (TBD) ـ في وجود كحولات خطية مختلفة. ومن خلال توضيح تأثيرات القواعد المهيمنة وسلوكيات المذيبات المصاحبة الكحولية التآزرية عبر تكوينات البنية الإلكترونية عالية المستوى، يقدم هذا العمل رؤى جزيئية حاسمة وضرورية للتصميم العقلاني وتحسين المذيبات العضوية عالية الأداء للحد الفعال من ملوثات كبريتيد الكربونيل.

**الكلمات المفتاحية** :احتجاز كبريتيد الكربونيل(COS) ؛ السوائل العضوية الرابطة(COS-BOLs) ؛ نظرية الدالة الكثافية (DFT)؛ الحركية ثلاثية الجزيئات؛ ارتباط الإلكترونات؛ تحلية الغاز.

## I. AN INTRODUCTION

In recent decades, natural gas has emerged as a cornerstone of the global energy matrix, driving the transition toward cleaner energy alternatives by progressively replacing coal and fuel oil. However, the sustainable exploitation of natural gas, particularly from highly contaminated or unconventional reserves, heavily relies on advanced gas processing technologies. Raw natural gas typically contains substantial amounts of acid gases and hazardous sulfur species. While the removal of hydrogen sulfide ($H_2S$) to meet strict pipelines and safety limits (typically below 5.7 $mg/m^3$) has been extensively optimized, commercial gas sweetening processes face critical challenges regarding trace sulfur contaminants [1-2].

Amid tightening environmental regulations, standard industrial specifications now restrict total sulfur content rather than merely $H_2S$. Consequently, eliminating less reactive sulfur compounds such as carbon disulfide ($CS_2$), mercaptans, and carbonyl sulfide COS has become equally paramount. Among these, COS represents a persistent threat; it is highly toxic, capable of severely poisoning industrial catalysts, and induces aggressive corrosion in pipelines and process equipment [2-5].

Reactive absorption utilizing alkanolamines or specialized organic solvents remains the industry standard for acid gas treating. Nevertheless, capturing (COS) efficiently requires a deeper molecular understanding of its reaction kinetics and thermodynamics, which are often obscured in macro-scale engineering studies. To bypass these limitations, Carbonyl Sulfide-Binding Organic Liquids (COS-BOLs) composed of hindered organic bases and linear alcohols have been proposed as highly efficient, tunable solvents. Yet, the exact mechanistic pathways, the prominent base effects, and the termolecular reaction kinetics governing these systems remain poorly understood at the quantum mechanical level [6-10].

To unveil the foundational factors driving this capture mechanism, this study deploys rigorous electron correlation methods to systematically investigate the efficiency of (COS) immobilization by organic solvent mixtures. Specifically, we explore the termolecular reaction kinetics and one-step reaction mechanisms between (COS) and key amidine or guanidine organic bases, including 1,8-diazabicycloundec-7-ene (DBU), 1,5-diazabicyclonon-5-ene (DBN), 2-tert-butyl-1,1,3,3-tetramethylguanidine (BTMG), and 1,5,7-triazabicyclodec-5-ene (TBD), in the presence of various linear alcohols. By analyzing the dominant base effects and alcohol co-solvent behaviors through high-level electronic structure calculations, this work delivers crucial molecular-level insights required to optimize and discover high-performance organic solvents for effective (COS) mitigation.

- **Quantum Mechanics**

Quantum mechanics calculations are used for clarifying the reaction mechanism, and highlighting the processes involved in it . This is a benefit because it allows the opportunity to calculate chemical properties with or without experimental data. Recently, quantum mechanics has improved in terms of calculations and applications pertaining to computational chemistry, and such calculations have been successfully applied to research for assessing the molecular structures, reaction mechanisms, and spectroscopic characterizations and thermodynamics of the studied systems. The mathematical expression for dynamical equations for particle velocity and mass are subdivided into four regimes Figure 1 [1-2].

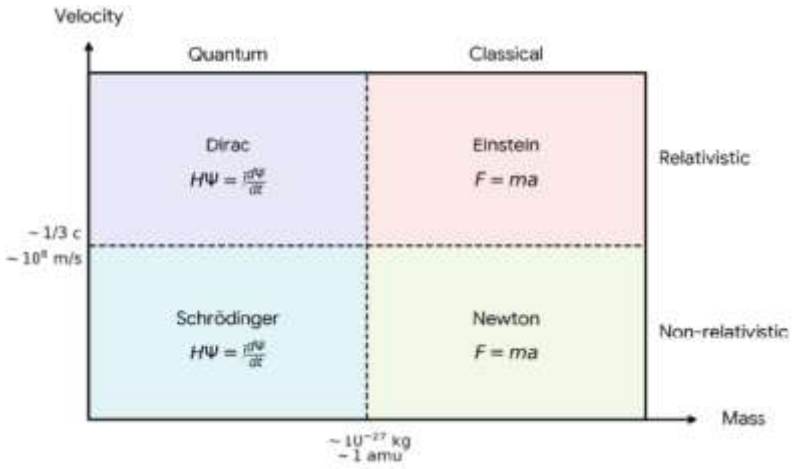


Figure 1: Domains of the dynamical equations [2].

The classic approach is very different when compared to quantum mechanics, because the later just explains approximations or probabilities, while the former is thought to be deterministic. The probability function is determined by taking the square of the wave function, as shown below.

Here, **r** represents the location/position, while *t* shows the time, and the wave function is denoted by $\Psi$, which is computed by solving the Schrödinger or Dirac equation (Figure 1) [1-2].

$$P\ (\mathbf{r}, t) = \ \Psi^2\ (\mathbf{r}, t).$$

$$H\Psi = E\Psi.$$

$$H\ \Psi_i(X_1, X_2, \dots, X_N, R_1, R_2, \dots, R_M) = E_i\Psi_i(X_1, X_2, \dots, X_N, R_1, R_2, \dots, R_M).$$

$$H = -\frac{1}{2}\sum_{i=1}^{N}\nabla_i^2 - \frac{1}{2}\sum_{A=1}^{M}\frac{1}{M_A}\nabla_A^2 - \sum_{i=1}^{N}\sum_{A=1}^{M}\frac{Z_A}{r_{iA}} + \sum_{i=1}^{N}\sum_{j>i}^{N}\frac{1}{r_{ij}} + \sum_{A=1}^{M}\sum_{B>A}^{M}\frac{Z_A Z_{AB}}{R_{AB}}.$$

$$\langle O\rangle = \int\dots\int \Psi_{trial}^{*}\ O\ \Psi_{trial}\ \mathrm{d}\vec{\mathrm{x}}_1\mathrm{d}\vec{\mathrm{x}}_1\dots\mathrm{d}\vec{\mathrm{x}}_1 \equiv \langle\Psi_{trial}|O|\Psi_{trial}\rangle.$$

$$H\Psi\ =\ i\frac{\partial\Psi}{\partial t}.$$

The Hamiltonian operator sums up all kinetic (*T*) and potential (*V*) energies.

$$H_{Schrodinger} = T + \ V$$

$$H\Psi\ =\ i\frac{\partial\Psi}{\partial t}$$

Here, the Hamiltonian operator is more complex.

$$H_{Dirac} = (c\alpha.\,\mathrm{p} + \beta mc^2) + V$$

Both α and β exist in the form of 4 × 4 matrices, while the relativistic wave function is made up of 4 components that are both large and small, and each one of them has $\alpha$ and $\beta$ spin functions that differ from the α and β matrices. Here, wave functions have two components: electronic (large components) and positronic (small components), wheras the α and β matrices couple components such as these. When the limit $c\rightarrow\infty$, the Schrödinger equation forms when Dirac equation is reduced; hence, the wave function components are reduced into the $\alpha$ and $\beta$ spin orbitals [1]. Although the Schrödinger equation is accurate, it is over-complicated, that a $H_2$ atom is the greatest system it can analytically solve. For calculating the multi-particle system, Dirac and others conducted several approximations [11].

- **Electron Correlation Methods**

**Density Functional Theory Foundations**

The Hartree-Fock Self-Consistent Field (HF-SCF) framework suffers from a fundamental deficiency due to its reliance on the mean-field approximation. By assuming that each electron moves within an average potential generated by all other electrons, the instantaneous position of any specific electron is treated as statistically independent of the remaining electronic coordinates. This approach fails to account for instantaneous inter-electron Coulombic repulsions, which in reality cause electrons to dynamically avoid one another. To recover this missing electron correlation in quantum chemical modeling, modern investigations rely heavily on Density Functional Theory (DFT) and Møller–Plesset perturbation theory (MP). For the present study of carbonyl sulfide (COS) capture kinetics, DFT offers an ideal balance of computational efficiency and accuracy by shifting the focus from the complex, 3N-dimensional many-body wavefunction to physically observable quantities principally the ground-state electron density, p(r). Figure 2. Conceptual flowchart outlining the systematic transition from uncorrelated wavefunctions to exact electronic density grids. (I) The mean-field limits of Hartree–Fock theory; (II) The conversion to physical ground-state electron density metrics via Hohenberg–Kohn mapping; and (III) Practical execution via non-interacting Kohn–Sham reference states to capture exchange-correlation profiles [12-14].

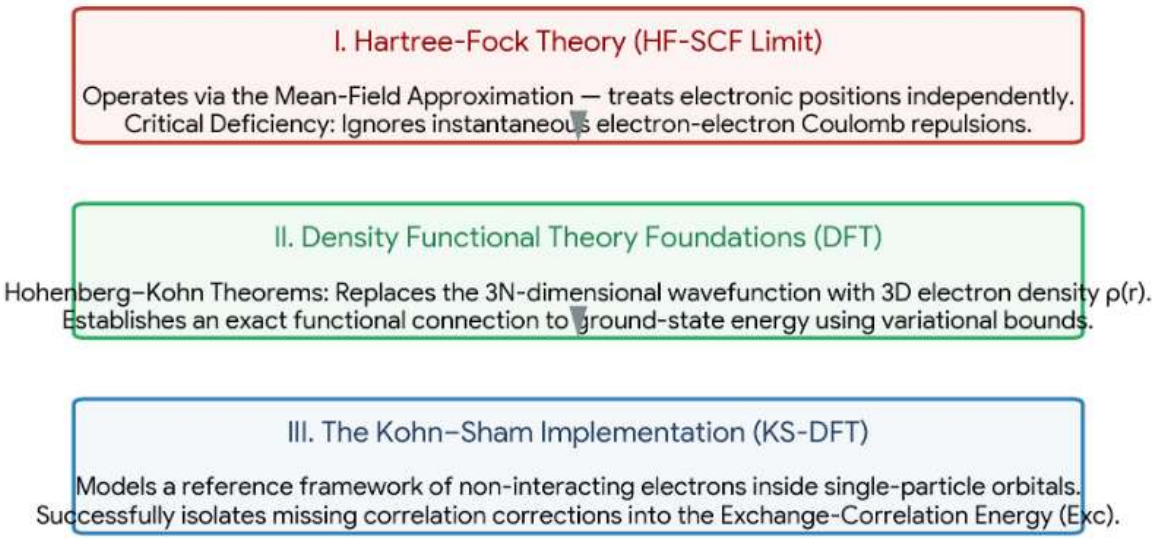


Figure 2: Methodological workflow of electron correlation methods and DFT foundations.

The electronic Hamiltonian of an N-electron system is uniquely determined by the total number of electrons, (N), and the external potential, $V_{ext}(r)$, exerted by the nuclei. Because p(r) integrates directly to the total number of electrons and exhibits local maxima precisely at the nuclear coordinates, it contains all the necessary structural parameters to completely reconstruct the system Hamiltonian. Mathematically, for an (N)-electron system in a given quantum state, the electron density $p(r_1)$ is derived by integrating the squared modulus of the many-body

wavefunction over the spin coordinates of the first electron and all spatial and spin coordinates of the remaining (N-1) electrons: The non-negative simple function shows the total number of electrons (*N*) [1-2]:

$$\rho(\mathbf{r_1}) = N \int_1 \ldots \int_N |\Psi(X_1, X_2, \ldots, X_N)|^2 ds_1 dx_2 \ldots dx_N.$$

$$N = \int \rho(\mathbf{r}) d\mathbf{r}.$$

$$E_{0a} < \int (\mathrm{V_a}(\mathbf{r}) - \mathrm{V_b}(\mathbf{r}))\, \rho_0(\mathbf{r}) d\mathbf{r} + \mathrm{E_{0b}}.$$

Here, no difference exists between *a* and *b*, so Eq. will become:

$$E_{0b} < \int (\mathrm{V}_b(\mathbf{r}) - \mathrm{V}_a(\mathbf{r}))\, \rho_0(\mathbf{r}) d\mathbf{r} + \mathrm{E}_{0a}.$$

$$\begin{aligned} E_{0a} + E_{0b} &< \int (\mathrm{V}_b(\mathbf{r}) - \mathrm{V}_a(\mathbf{r}))\, \rho_0(\mathbf{r}) d\mathbf{r} + \int (\mathrm{V}_a(\mathbf{r}) - \mathrm{V}_b(\mathbf{r}))\, \rho_0(\mathbf{r}) d\mathbf{r} + E_{0b} + \mathrm{E}_{0a} \\ &< \int (\mathrm{V}_b(\mathbf{r}) - \mathrm{V}_a(\mathbf{r}) + \mathrm{V}_a(\mathbf{r}) - \mathrm{V}_b(\mathbf{r})) \rho_0(\mathbf{r}) d\mathbf{r} + E_{0b} + \mathrm{E}_{0a} \end{aligned}$$

$< E_{0b} + \mathrm{E}_{0a}$.

This means that there is a contradiction [1-2]:

$E_{0a} + \mathrm{E}_{0b} < E_{0b} + \mathrm{E}_{0a}\ or\ 0 < 0.$

Kohn and Sham (KS) used the HF theory to bring the HK theorems into reality, and performed its calculations. It is necessary to develop the required imaginary system for *N* non-interacting electrons with the density of a real system. This system has a ground state wave function $\Psi_0$ that has been expressed through a single-slater determinant. This slater determinant is formed by the KS orbital (ϕKS) to solve *N* single-particle equations. The ϕKS variations determine the energy and density of the ground state on the basis of the variational principle.

The single-electron KS operator is given below [1-12]:

$$h_i^{KS} = -\frac{1}{2}\nabla_i^2 - \sum_k^{nuclei} \frac{Z_k}{|r_i - r_k|} + \int \frac{\rho(r')}{|r_i - r'|} dr' + V_{xc}$$

$$V_{xc} = \frac{\delta E_{xc}}{\delta \rho}.$$

Here, $E_{xc}$ is the $V_{xc}$ expectation value and $V_{xc}$ is a single-electron operator. The KS-energy contribution comes from the exchange correlation energy ($E_{XC}$), which includes the kinetic energy corrections, which emerge because of electron-electron repulsions, while the interaction correlations need corrections [1-2].

## II. RESULTS AND DISCUSSION

**Geometrical Evolution and Termolecular Capture Mechanism:** To unveil the microscopic efficiency of carbonyl sulfide (COS) immobilization, the geometric parameters of the reactants (R), transition states (TS), and products (P) were systematically evaluated. The termolecular, single-step reaction mechanisms involving organic bases (DBU, DBN, BTMG, and TBD) and linear alcohols (methanol, ethanol, 1-propanol, 1-butanol, 1-pentanol, and 1-hexanol) were mapped using long-range corrected hybrid density functional theory with empirical dispersion (ωB97X-D3/6-311++G(d,p)). This advanced electron correlation method accurately captures the delicate interplay of non-covalent interactions and charge re-distribution governing the capture matrix. Key structural parameters tracking this single-step transformation are detailed in Table 1. The capture efficiency is fundamentally driven by a synchronized proton-transfer and nucleophilic attack pathway. In the reactant complex, the alcohol hydroxyl group acts as a bridge between the organic base and the (COS) molecule. At the un-isolated reactant stage, weak hydrogen bonding between the nitrogen atom (N1) of the organic base and the hydroxyl hydrogen (H31) of the alcohol induces a slight elongation of the (H31–O26) bond compared to its isolated form (0.956A). For instance, in the (COS/BTMG/methanol) reactant assembly, the (H31–O26) distance stretches to (0.990A), dictated by the unshared electron pair on (N1).

Figure 3: Schematic representation of the termolecular reaction scheme for carbonyl sulfide immobilization.

As the system progresses over the activation barrier to the transition state, the (H31–O26) bond breaks as a consequence of the strong attractive force exerted by the (N1) center. Concurrently, a new covalent (N1–H31) bond forms. This structural migration is reflected by the steady reduction of the (H31–N1) distance across all systems, collapsing from an average of (1.76A°) down to (1.02A°) in the product complexes (Table 1).

Simultaneously, the deprotonated oxygen (O26) targets the electrophilic carbon (C25) of (COS), converting the linear molecule into a bent thiocarbonate derivative. Isolated (COS) maintaining a strictly linear conformation (180°) undergoes modest initial bending (2)–(2.3) in the reactant stage

due to weak early phase (O26-C25) interactions. During the transition state, severe geometric deformation takes place as the (O27–C25–S28) angle contracts rapidly to values near (150°). In the final bound product state, the (O27–C25–S28) bond angle stabilizes at (128°), while the newly formed (C25–O26) covalent distance shortens dramatically to (1.38A). Table shown the optimized geometric parameters (bond lengths in (Å) and angles in degrees) tracking the active structural evolution of (COS) capture complexes calculated at the ωB97X-D3/6-311++G(d,p) level.

Table 1: Optimized geometric parameters

| **System Matrix** | **State** | **(H31–N1) Å** | **(H31–O26) (Å)** | **(C25–O26) (Å)** | **(C25–O27) (Å)** | **(C25–S28) (Å)** | **(O27–C25–S28) (◦)** |
|---|---|---|---|---|---|---|---|
| **(COS/DBU/methanol)** | R | 1.763 | 0.989 | 3.041 | 1.152 | 1.563 | 177.88 |
| | TS | 1.386 | 1.109 | 1.917 | 1.170 | 1.621 | 150.02 |
| | P | 1.017 | 1.972 | 1.382 | 1.220 | 1.723 | 128.17 |
| **COS/DBU/ethanol)** | R | 1.765 | 0.989 | 3.076 | 1.152 | 1.563 | 178.03 |
| | TS | 1.427 | 1.087 | 1.893 | 1.171 | 1.624 | 149.25 |
| | P | 1.018 | 1.937 | 1.384 | 1.220 | 1.723 | 127.96 |
| **(COS/DBU/1-propanol)** | R | 1.780 | 0.988 | 3.160 | 1.152 | 1.562 | 178.10 |
| | TS | 1.424 | 1.089 | 1.891 | 1.171 | 1.624 | 149.26 |
| | P | 1.017 | 1.951 | 1.386 | 1.220 | — | — |

As shown in Figure 4, the compact methyl group in the methanol reactant complex (R) provides minimal steric hindrance. This allows for optimal spatial alignment, positioning the nucleophilic oxygen (O26) within (3.041A) of the electrophilic carbon (C25), which initiates a (2.1) bending of the linear (COS) core. At the transition state (TS), the (H31–O26) bond breaks (1.109A) while the forming (C25…O26) bond contracts to (1.917A), bending the (O27–C25–S28) angle to (150.02). This smoothly yields a stable chemisorbed product (P) with a covalent (C25–O26) bond of (1.382A) and a relaxed angle of (128.17). Conversely, Figure 5 visually demonstrates the severe steric blockades imposed by longer aliphatic chains. In the 1-hexanol reactant complex (R), the bulky six-carbon chain disrupts spatial proximity, expanding the initial (C25…O26) separation beyond (4.3A). This wide gap suppresses early phase interactions, restricting the initial bending of the (COS) frame to a mere (0.3). Consequently, the system requires a demanding structural reorganization to fold the hexyl chain at the transition state. While the final product (P) achieves a comparable covalent bonding profile (1.385A), (128.23), the initial structural resistance detailed in Figure 5 confirms that increasing the co-solvent chain length severely limits early-stage capture efficiency. Figure 6 shown the steric effect constraints on the geometrical parameters of carbonyl sulfide reactant complexes.

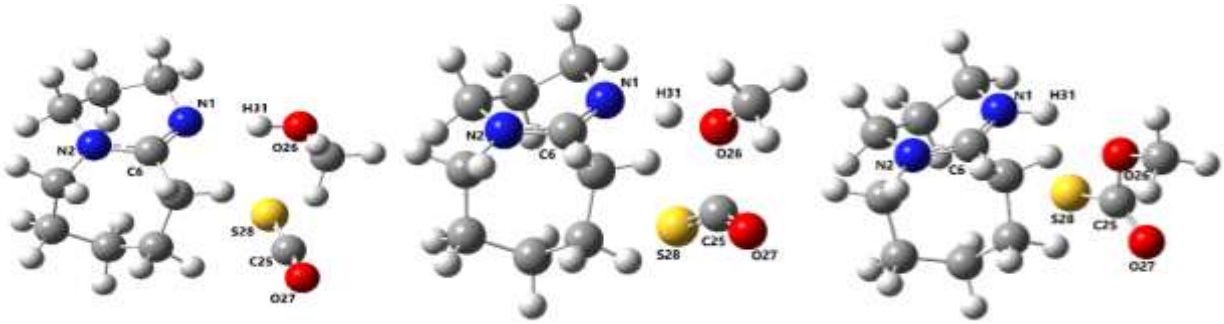


Figure 4: R (top), TS (middle), and P (bottom) structures of the COS/DBU/methanol system.

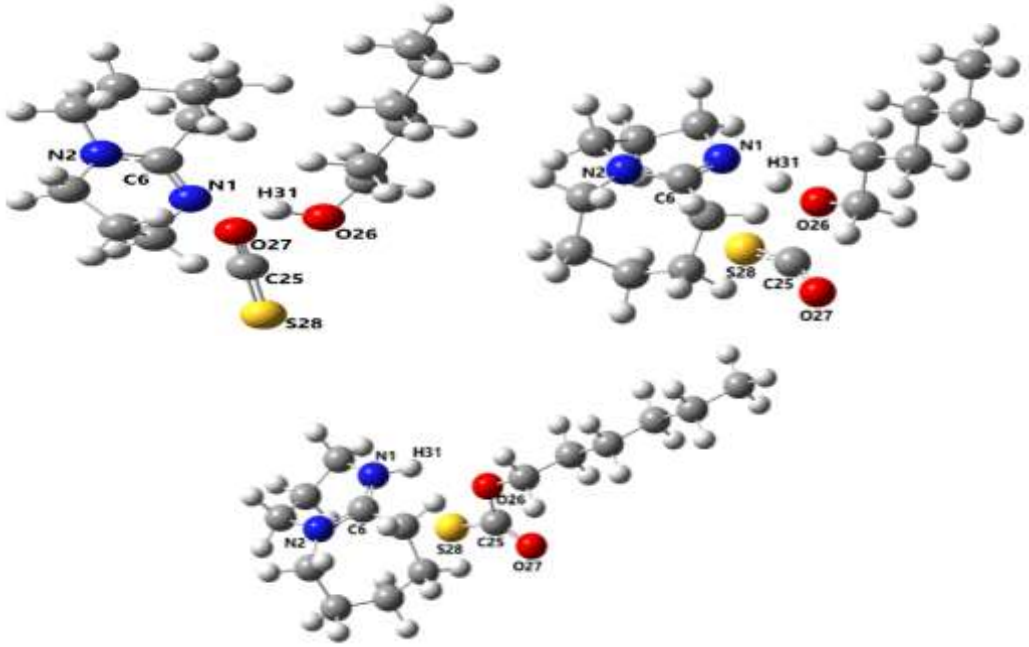


Figure 5: R (top), TS (middle), and P (bottom) structures of the COS/DBU/1-hexanol system.

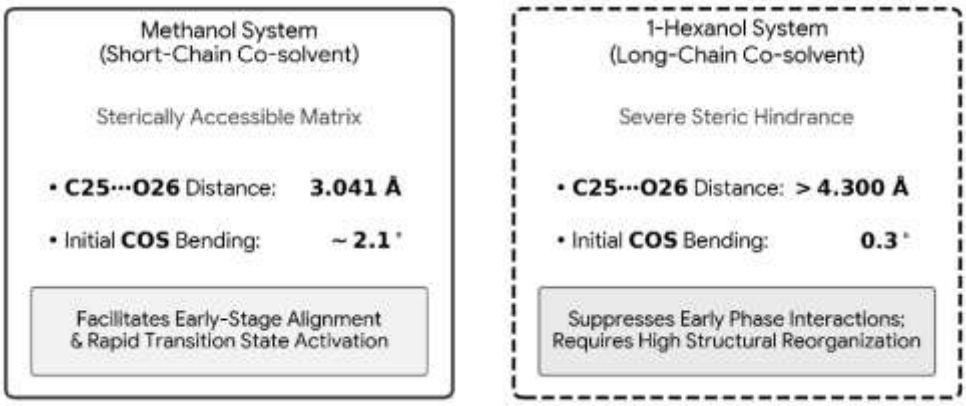


Figure 6: Steric effect constraints on the geometrical parameters of carbonyl sulfide reactant complexes.

## III. CONCLUSIONS

In this study, high-level electronic structure calculations utilizing long-range corrected hybrid density functional theory with empirical dispersion corrections (ωB97X-D3/6-311++G(d,p)) were deployed to unveil the mechanistic efficiency of carbonyl sulfide (COS) capture by organic solvent systems. The rigorous quantum chemical modeling of the single-step termolecular reaction pathway yielded several critical insights:

Synchronized Reaction Mechanism: The immobilization of (COS) by mixtures of hindered organic bases (DBU, DBN, BTMG, and TBD) and linear alcohols operates via a highly synchronized, single-step termolecular mechanism. This path features a simultaneous proton transfer from the alcohol hydroxyl group (H31–O26) to the basic nitrogen center (N1), coupled with a nucleophilic attack from the deprotonated oxygen (O26) to the electrophilic carbon (C25) of (COS). Geometrical Evolution as Efficiency Indicators: The High-precision electron correlation method tracked a profound geometric transformation, where the isolated linear structure of (COS) (180◦) shifts down to a highly bent conformation (150) at the transition state and (128) in the bound thiocarbonate product). This severe bending, combined with the dramatic contraction of the newly formed (C25–O26) covalent bond to (1.38A), serves as a clear structural marker of successful chemical capture. Steric Constraints of Co-solvents: Aliphatic chain lengths of linear alcohols impose prominent steric blockades. While shorter-chain alcohols (like methanol) facilitate close spatial alignment and early-stage activation in the reactant complex, longer-chain co-solvents (1-butanol, 1-pentanol, and 1-hexanol) expand the initial (C25–O26) separation beyond (4.3A) and suppress early (COS) bending to a mere (0.3), thereby lowering the structural capture efficiency. Overall, this investigation demonstrates that combining sterically accessible organic bases with highly mobile, short-chain linear alcohols offers the most efficient liquid matrix for gas sweetening processes. The molecular-level data provided by this electron correlation study establish a solid theoretical baseline for designing next-generation, high-performance (COS)-binding organic liquids (COS-BOLs).

## REFERENCES

1. Abduesslam, M. (2026). Theoretical investigation of carbonyl sulfide capture by organic solvents [Master's thesis, Atılım University]. Graduate School of Natural and Applied Sciences.
2. Abduesslam, M., & Ramadan, N. (2026). Theoretical investigation into the capture mechanism of carbonyl sulfide by organic solvents: An ab initio quantum chemical approach. Surman Journal for Science and Technology, 8(2), 544–559.
3. F. Jensen, Introduction to Computational Chemistry. Wiley, 2016, pp. 664.
4. R.G. Parr, “Density Functional Theory of Atoms and Molecules”, In: Fukui K., Pullman B. (eds) Horizons of Quantum Chemistry. Académie Internationale Des Sciences Moléculaires Quantiques / International Academy of Quantum Molecular Science, vol 3. Springer, Dordrecht. 1980.
5. W. Koch and M.C. Holthausen, A chemist’s Guide to Density Functional Theory. Wiley-VCH, 2001.

6. E.F. da Silva, "Computational Chemistry Study of Solvents for Carbon Dioxide Absorption." Ph.D. thesis, Fakultet for Naturvitenskap Og Teknologi, 2005.
7. Barreau, E. Blanchon Le Bouhelec, K. N. Habchi Tounsi, P. Mougin and F. Lecomte, "Absorption of $H_2S$ and $CO_2$ in Alkanolamine Aqueous Solution: Experimental Data and Modelling with the Electrolyte-NRTL Model", Oil & Gas Science and Technology, vol. 61, no. 3, pp. 345–361, 2006.
8. Maiuf, A., & Ramadan, N. (2024). The acetic acid production by modeling oxidation of ethylene with Aspen Plus. Surman Journal of Science and Technology, 6(2), 139–149.
9. K. Othmer, "Metathesis" in Encyclopedia of Chemical Technology, vol. 26. J. Peters, Ed. New York: McGraw-Hill, 2005, pp. 920–958.
10. F. Amararene and C. Bouallou, "Kinetics of Carbonyl Sulfide (COS) Absorption with Aqueous Solutions of Diethanolamine and Methyldiethanolamine", Industrial and Engineering Chemistry Research, vol. 43, no. 19, pp. 6136–6141, 2004.
11. G. Hinderaker and O.C. Sandall, "Absorption of Carbonyl Sulfide in Aqueous Diethanolamine", Chemical Engineering Science, vol. 55, no. 23, pp. 5813–5818, 2000.
12. S.C. Lee, M.J. Snodgrass, M.K. Park and O.C. Sandall, "Kinetics of Removal of Carbonyl Sulfide by Aqueous Monoethanolamine", Environmental Science and Technology, vol. 35, no. 11, pp. 2352–2357, 2001.
13. F. Yan, R. Kakuchi, K. Takahashi and H.J. Kim, "$CS_2$ Capture in the Ionic Liquid 1-alkyl-3-methylimidazolium Acetate: Reaction Mechanism and Free Energetics", Physical Chemistry Chemical Physics, vol. 20, no. 29, pp. 19339–19349, 2018.
14. P.D. Vaidya and E.Y. Kenig, "Kinetics of Carbonyl Sulfide Reaction with Alkanolamines: A review", Chemical Engineering Journal, vol. 148, no. 2–3. pp. 207–211, 2009.